Kinetic Analysis of Transcytosis of Epidermal Growth Factor in Madin-Darby Canine Kidney Epithelial Cells

Akiko Kozu,[1] Yukio Kato,[1] Yoshihisa Shitara,[1] Manabu Hanano,[2] and Yuichi Sugiyama[1,3]

Received January 13, 1997; accepted May 27, 1997

Purpose. The aim of this study is to clarify the intracellular fate and a rate limiting step in transcytosis of epidermal growth factor (EGF) in Madin-Darby Canine Kidney (MDCK) epithelial cells.

Methods. The kinetics of transcytosis of ^{125}I-EGF was investigated. To examine the fate of EGF molecules bound to its receptor on the cell surface, ^{125}I-EGF was prebound to the basal surface at 4°C, followed by extensive washing and subsequent incubation at 37°C in EGF-free medium.

Results. Saturable transport of ^{125}I-EGF through the cell monolayer could only be observed from the basal to apical side. Most (~90%) of the EGF molecules bound to the surface receptor are internalized with a half-life of 1–3 min, followed by intracellular degradation with a half-life of 20–50 min. The exocytosis of internalized EGF into the apical medium is much slower with a half-life of 130–250 min. Even when ^{125}I-EGF was incubated with MDCK cells at 37°C and washed with acid to remove cell-surface ^{125}I-EGF, intact ^{125}I-EGF appeared in the basal medium with a half life of 160–170 min.

Conclusions. The exocytosis of internalized EGF into the apical medium is a rate limiting step in EGF transcytosis. At least a small amount of internalized EGF is recycled.

KEY WORDS: epidermal growth factor; receptor-mediated endocytosis; transcytosis; Madin-Darby Canine Kidney (MDCK) epithelial cell.

INTRODUCTION

Receptor-mediated endocytosis is used as a target of drug delivery system (DDS) to allow therapeutic agents with a limited membrane permeability, such as genes and toxins, to be delivered to a specific target cell (1–3). Since, in epithelial cells, at least a small fraction of endocytosed ligand is transported to the opposite side of the cell (transcytosis) (4–6), RME can also be used to increase the absorption of therapeutic agents with low systemic absorption when the RME in epithelial cells in several organs, such as lung and intestine, is a target. Transcytosis in brain capillary endothelial cells is one of the most promising ways for targeting drugs to the brain (3). However, most of the internalized ligand is generally transferred to lysosomes and subsequently degraded by hydrolases. To construct an efficient delivery system, it is necessary to regulate the intracellular fate of the ligand.

[1] Faculty of Pharmaceutical Sciences, University of Tokyo, 7-3-1 Hongo, Bunkyo-ku, Tokyo 113, Japan.

[2] Faculty of Pharmaceutical Sciences, Nihon University, Narashinodai, Funabashi-shi, Chiba 274, Japan.

[3] To whom correspondence should be addressed.

ABBREVATIONS: EGF, Epidermal growth factor; RME, Receptor-mediated endocytosis; MDCK cell, Madin-Darby Canine Kidney cell; BSA, Bovine serum albumin; TCA, trichloroacetic acid.

Although drug targeting via RME has succeeded in both in vivo and in vitro experimental models (1–3), most of the studies have only analyzed the input (administration of DDS) and output (pharmacological effect). However, to achieve an optimally efficient drug targeting system, it is also important to analyze the kinetics of the administered DDS in the body. Considering the importance of the intracellular fate of DDS targetted to RME, in the present study, we have attempted to establish experimental models for analyzing the intracellular kinetics of the ligand involving transcytosis through epithelial cells.

Madin-Darby Canine Kidney (MDCK) cells are widely used as an in vitro experimental system to investigate transcellular transport (4–6). We used an MDCK cell monolayer as a model for epithelial cells. Since MDCK cells express the EGF receptor (4,6), cellular handling of EGF was analyzed as a model ligand for RME. In MDCK cells, unidirectional transport of EGF from the basal to apical side has been previously reported (4). To understand the reason for such unidirectional transport, we have to note that such vectorial transcellular transport can be affected not only by the cell-surface receptor density, but also by cell-surface sorting due either to dissociation or internalization, and intracellular sorting due either to lysosomal degradation or transcytosis. In the present study, to investigate the rate-limiting step for the transcellular transport, we investigated the kinetics of the sequential processes in the transcytosis of EGF.

MATERIALS AND METHODS

Materials

Recombinant human EGF was a gift from Wakunaga Pharmaceutical Co. Ltd. EGF was radioiodinated by the chloramine-T method as reported elsewhere (7).

Cell Culture

MDCK cells (American Type Tissue Collection, Rockville, MD) were cultured in Dulbecco's Modified Eagle Medium (Nikken Biomedical Laboratories, Kyoto) supplemented with 10% Fetal Bovine Serum (GIBCO/BRL Life Technologies Inc., NY) and 0.005% Streptomycin (Wako Pure Chemical, Osaka) at 37°C in 5% CO_2 (5). Passages 59–81 were used in this study. Within 4 days the cells reached confluence and were passaged as described elsewhere (5). Monolayers of polarized epithelial cells were produced by seeding the cells in Cell Culture Inserts (pore size 3.0 μm; FALCON/Beckton Dickinson Labware, Franklin Lakes, NJ) with 2.8×10^4 cells for 6.25 mm (0.31 cm^2) filters. Two days after seeding, cells were refed. Experiments were conducted 4 days after seeding to allow the development of tight junctions and a polarized phenotype. Before experiments, cells were washed with an incubation volume (apical side; 0.3 ml, basal side; 0.9 ml) of transport buffer, which consisted of Hanks' solution (GIBCO/BRL Life Technologies, Inc. Grand; Island NY) buffered with 20 mM HEPES (Wako Pure Chemical, Osaka) at pH 7.2 supplemented with 0.2% BSA (SIGMA, St. Louis, MO). We used only cell monolayers with electrical conductivity over the range 120–1020 Ωcm^2.

0724-8741/97/0900-1228$12.50/0

Transcytosis of ^{125}I-EGF

Both ^{125}I-EGF (0.610 μCi/ml) and ^{14}C-inulin (0.947 μCi/ml, New England Nuclear, Boston, MA) were simultaneously added to the basal or apical side of the MDCK cell monolayer and cells were incubated at 37°C. At designated times, either basal or apical medium containing transcytosed ^{125}I-EGF was collected, and the same volume of ligand-free buffer prewarmed to 37°C was added to the monolayer. The sample (0.1 ml) for the determination of ^{125}I-EGF was mixed with 0.4 ml ice-cold transport buffer and also 0.5 ml 20%(w/v) trichloroacetic acid (TCA), and allowed to stand for 5 min on ice, followed by centrifugation for 1 min using a table-top microfuge (Beckman Instruments, Fullerton, CA). The radioactivity in the precipitate was determined.

^{125}I-EGF Binding Assay

^{125}I-EGF (0.638–1.04 μCi/ml, 0.507–0.737 nM) was added to the basal or apical side of the MDCK cell monolayer in the presence of unlabeled EGF (0–100 nM). Binding of ^{125}I-EGF to the MDCK cells was determined at 4°C for 2 h. 0.1 ml apical or basal medium was collected to measure the unbound ^{125}I-EGF and cells were rinsed six times with an incubation volume of ice-cold transport buffer. An incubation volume of ice-cold Hanks' solution buffered with MES (pH 3.0) supplemented with 0.2% BSA (acid buffer) was added to both basal and apical sides and allowed to stand for 10 min on ice. This treatment dissociates at least 90% of the receptor-bound ^{125}I-EGF molecules. After 10 min, buffer was collected and washing with the same volume of ice-cold acid buffer was repeated. Both washes from each side were combined and their radioactivity was determined as acid-washable (surface-bound) ^{125}I-EGF.

Pulse-Chase Study 1

^{125}I-EGF (0.596–1.29 μCi/ml, 0.450–0.746 nM) was added to the basal side of the MDCK cell monolayer, followed by incubation at 4°C for 2 h. Following incubation, the cell monolayer was washed six times and then incubated in ligand-free buffer at 37°C. At designated times, both TCA-precipitable and TCA-soluble radioactivity and surface-bound ^{125}I-EGF were determined as described above. 0.9 ml PBS (pH 7.4) containing 0.5% Triton X-100 (lysing buffer) was added to the cell monolayer and allowed to stand at 4°C overnight. The cell lysate obtained was combined with 0.06 ml PBS, 0.12 ml 1% (w/v) BSA solution and 0.12 ml 100% (w/v) TCA solution, and allowed to stand for 5 min on ice. After centrifugation, the radioactivity in the supernatant (TCA-soluble radioactivity inside the cells) and precipitates (acid-resistant and TCA-precipitable radioactivity) was determined as the degradation product inside the cells and internalized ^{125}I-EGF, respectively. Unlabeled EGF (50 nM) was premixed with ^{125}I-EGF to determine the nonspecific EGF transport, which was found to be less than 10% of the total EGF transport. To more precisely examine the internalization and dissociation of EGF prebound to its receptor, the chase times were changed to 0, 1, 3, 5, and 10 min in a different set of experiments.

Pulse-Chase Study 2

^{125}I-EGF (0.596–1.29 μCi/ml, 0.450–0.746 nM) was added to the basal side of the MDCK cell monolayer. After incubation at 4°C for 2 h, the cell monolayer was washed six times and incubated in EGF-free buffer at 37°C for 10 min. After another six washings, ice-cold Hanks' solution buffered with MES (pH 4.0) supplemented with 0.2% BSA (mild acid buffer) was added to remove surface-bound ^{125}I-EGF. The cell monolayer was then washed once with ice-cold transport buffer and incubated in EGF-free medium at 37°C. At designated times, both surface-bound and internalized ^{125}I-EGF, and degradation product were determined as described above. Unlabeled EGF (50 nM) was premixed with ^{125}I-EGF to determine the nonspecific EGF transport, which was found to be less than 10% of total EGF transport.

Pulse-Chase Study 3

^{125}I-EGF (0.5 nM) was added to the basal side of the MDCK cell monolayer. After the incubation at 37°C for 20 min, the monolayer was washed four times with ice-cold transport buffer and once with mild acid buffer, and further incubated in EGF-free buffer at 37°C. At designated times, both surface-bound and internalized ^{125}I-EGF, and degradation product were determined. Unlabeled EGF (50 nM) was premixed with ^{125}I-EGF to determine the nonspecific EGF transport, which was found to be less than 10% of total EGF transport.

Binding Assay to Isolated Rat Liver Plasma Membrane

Plasma membrane was separated as reported previously (8) and stored in solution, 2 mg protein/ml, at −100°C. Either radioactive ligands released from the cell interior into the basal medium or authentic ^{125}I-EGF, dissolved in transport buffer, was incubated with the plasma membrane (final 0.5 mg protein/ml) on ice for 60 min in the presence or absence of excess (50 nM) unlabeled EGF. The final incubation volume was 0.1 ml. After incubation, the mixture was centrifuged at 15,000 rpm (Tomy MRX-152, Tokyo) at 4°C for 10 min. TCA-precipitable radioactivity in 0.05 ml supernatant was measured as the medium concentration (cpm/μl). The remaining supernatant was discarded and 1 ml ice cold incubation buffer was added, mixed and centrifuged at 15,000 rpm. Plasma membrane was washed twice using this method. The radioactivity in the final membrane precipitate (cpm/mg protein) was determined. Binding was normalized for the medium concentration and expressed as μl/mg protein.

Kinetic Analysis

Cell-surface ligand (LR_s) can be described by the well-known Langmuir equation (10):

$$[LR_s] = R_s[L]/(K_d + [L]) + \alpha[L] \quad (1)$$

where R_s, [L], K_d, and α are the density of free receptor on the cell-surface, the concentration of unbound ligand in the medium, an equilibrium dissociation constant, and the proportional constant for nonspecific binding, respectively. The K_d and R_s were estimated by fitting $[LR_s]$ and [L] to Eq. (1) by the nonlinear minimum squares method "MULTI" (9). When ligand was applied to the basal side, internalization rate constant (k_{int}), dissociation rate constant (k_{off}), transcytosis rate constant (k_{trans}), and degradation rate constant (k_{deg}) were estimated from the initial slope of a plot based on the following equations, respectively (10):

$$L_{int} = k_{int} \int_0^t [LR_{s,basal}]\, dt \quad (2)$$

$$[X_{basal}] = k_{off} \int_0^t [LR_{s,basal}]\, dt \quad (3)$$

$$[X_{apical}] = k_{trans} \int_0^t [L_{int}]\, dt \quad (4)$$

$$[L_{deg}] = k_{deg} \int_0^t [L_{int}]\, dt \quad (5)$$

where L_{int}, X_{basal}, X_{apical}, and L_{deg} were internalized ligand, ligand released into the basal medium, ligand released into the apical medium, and degradation product, respectively. $\int_0^t [LR_{s,basal}]\, dt$ and $\int_0^t [L_{int}]\, dt$ were estimated by the trapezoidal method. The recycling rate constant ($k_{recycle}$) was estimated using Eq. (6), in pulse-chase studies 2 and 3, where X_{basal} cannot be influenced by ligand dissociated from the cell-surface receptors:

$$[X_{basal}] = k_{recycle} \int_0^t [L_{int}]\, dt \quad (6)$$

RESULTS

Transcytosis

The cumulative amount of TCA-precipitable radioactivity appearing in the apical medium after the addition of a tracer quantity of ^{125}I-EGF to the basal medium was approximately twice that in the basal medium after addition to the apical medium (Fig. 1A). In the presence of excess (50 nM) unlabeled EGF, the TCA-precipitable radioactivity transferred from basal to apical medium was comparable with that from apical to basal medium (Fig. 1B). The TCA-precipitable radioactivity transferred from the basal to apical medium was reduced in the presence of excess unlabeled EGF in the basal medium (Fig. 1A, 1B). On the other hand, the effect of unlabeled EGF was minimal on the transcytosis from apical to basal medium (Fig. 1A, 1B). The transfer of ^{14}C-inulin from basal to apical medium was almost exactly the same as that from apical to basal medium (Fig. 1C). Transcytosis of ^{14}C-inulin both from basal to apical and from apical to basal was comparable with that of TCA-precipitable radioactivity in the presence of excess unlabeled EGF in the corresponding direction (Fig. 1B, 1C).

Saturation of Cell-Surface EGF Binding Both on Basal and Apical Surface Membrane

Specific binding was much higher on the basal surface than the apical one (Fig. 2A). Scatchard plots revealed that there is one saturable and one nonsaturable component for binding to both basal and apical membranes (Fig. 2B). The K_d was 1.44 ± 0.62, 0.716 ± 0.668 nM, and the R_s was 9.94 ± 2.27, 1.37 ± 0.56 fmol/well (mean ± calculated SD) for the basal and apical sides, respectively.

Fate of EGF Prebound to Its Receptor on the Basal Surface (Pulse-Chase Study 1)

After the MDCK cells were incubated at 4°C for 2 hours with a tracer amount of ^{125}I-EGF in the basal medium, the acid-washable radioactivity on the basal side was 4.86 ± 1.31 μl/well while the acid-resistant and TCA-precipitable radioactivity was only 0.350 ± 0.218 μl/well (Fig. 3C), when the radioactivity was normalized with respect to the initial concentration added to the basal medium. During the incubation in EGF-free medium, acid-washable radioactivity fell gradually while acid-resistant and TCA-precipitable radioactivity increased and then gradually decreased (Fig. 3A). TCA-precipitable radioactivity released into the basal medium also increased in a time-dependent manner although the amount at 10 min was approximately 1/10 that internalized (Fig. 3C). TCA-precipitable radioactivity

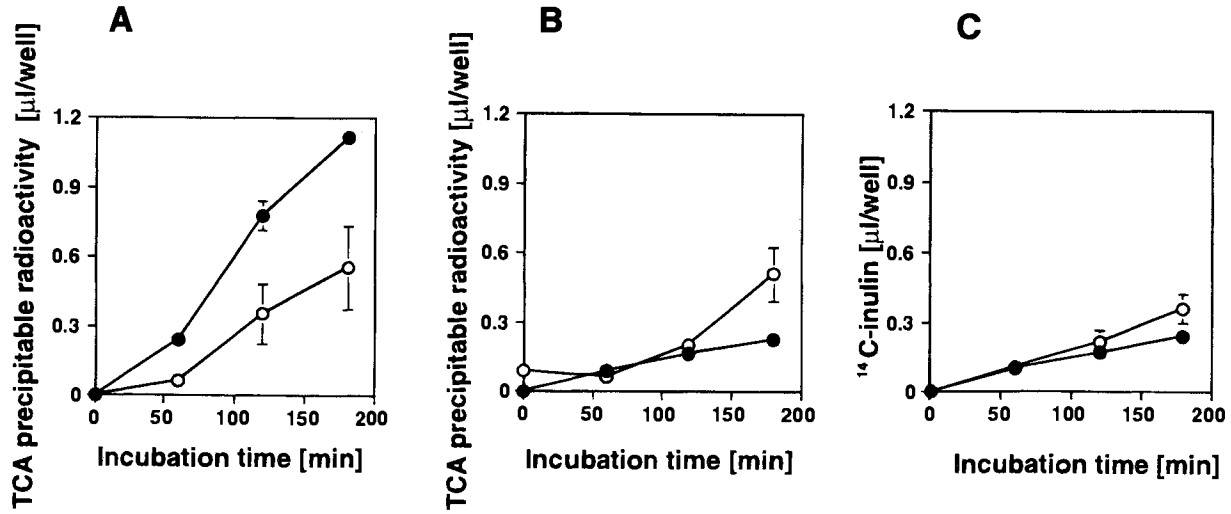

Fig. 1. Transcellular transport of ^{125}I-EGF and ^{14}C-inulin through MDCK epithelial cells. A tracer amount of ^{125}I-EGF with (panel B) or without (panel A) excess (50 nM) unlabeled EGF was applied either to the basal (●) or apical (○) medium, and TCA-precipitable radioactivity appearing in the medium on the opposite side was determined at designated times. Data are expressed as cumulative emerging amounts normalized with respect to the initial applied concentration in the medium. Each value represents the mean ± S.E. of three independent experiments. To estimate nonspecific transport, ^{14}C-inulin was also applied (panel C) and its transport determined.

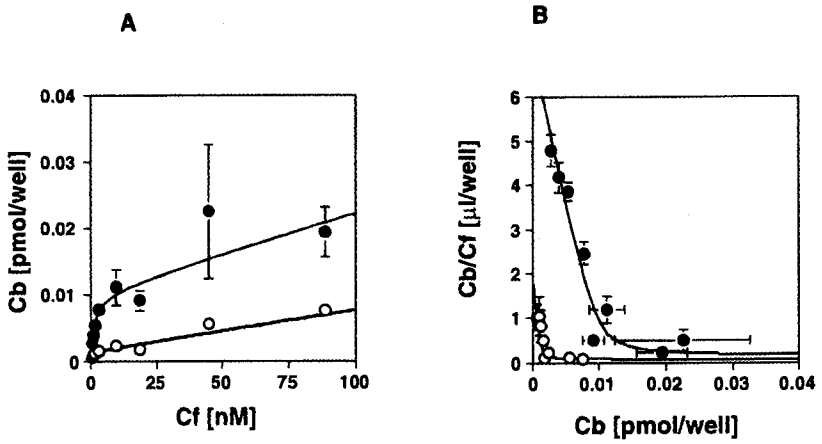

Fig. 2. Saturation of EGF binding on the surface of MDCK cells. A tracer amount of ^{125}I-EGF with various concentrations (0–100 nM) of unlabeled EGF was applied to either basal (●) or apical (○) side medium. Cell monolayer was incubated for 2 hours at 4°C. After extensive washing of each side, acid-washing was performed to determine the cell-surface ^{125}I-EGF binding. Data for the acid-washable binding shown in panel A were replotted in panel B as a Scatchard plot. Each value represents the mean ± S.E. of three independent experiments.

passing into the apical medium increased after a lag-time of at least 5 min, and its cumulative amount during a 2-hour incubation was 0.342 ± 0.055 μl/well (Fig. 3B). The acid-washable radioactivity on the apical side was virtually negligible at any of the times investigated (Fig. 3A).

Fate of Internalized EGF (Pulse-Chase Study 2)

The acid-resistant and TCA-precipitable radioactivity at the start of the chase period was 1.86 ± 0.24 μl/well and decreased with time (Fig. 4A). The degradation product increased in a time-dependent manner with a y-intercept of 0.800 ± 0.101 μl/well at the start of the chase period, which represents degradation product remaining inside the cells which could not be removed by washing with buffer. The degradation product reached 2.71 ± 0.20 μl/well after a 2-hour chase period (Fig. 4B). TCA-precipitable radioactivity appearing in the apical medium during the 2-hour chase period was 0.279 ± 0.073 μl/well, much less than the cumulative amount degraded (Fig. 4B). TCA-precipitable radioactivity also appeared in the basal medium, increasing in a time-dependent manner (Fig. 4B). As far as the appearing radioactivity was concerned, its binding to isolated plasma membrane was 0.318 μl/mg protein while that in the presence of excess (50 nM) unlabeled EGF was 0.231 μl/mg protein. On the other hand, the binding of authentic ^{125}I-EGF was 9.85 × 10^{-2} μl/mg protein while that in the presence of excess unlabeled EGF was 3.71 × 10^{-2} μl/mg protein. Specific binding, obtained by subtraction of the binding in the presence of excess unlabeled EGF from that under tracer

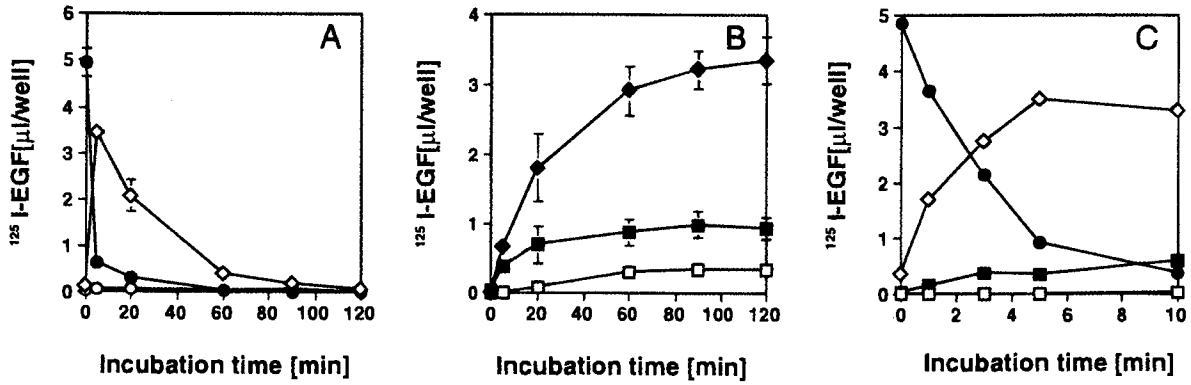

Fig. 3. Fate of EGF prebound to its receptor on the basal surface in MDCK cells (pulse-chase study 1). A tracer amount of ^{125}I-EGF was applied to the basal medium, followed by a 2-hour incubation at 4°C. After washing the cells with ice-cold transport buffer (pH 7.2), the prewarmed buffer was applied to the monolayer, and the cells were incubated at 37°C. At designated times, the TCA-precipitable radioactivity in basal (■) and apical (□) medium was determined (panel B). After washing the cells with buffer, the surface-bound ^{125}I-EGF on the basal (●) and apical (○) sides and internalized ^{125}I-EGF (◇) were determined by the acid washing technique (panel A). The TCA-soluble radioactivity in the cells and media were summed and shown as (◆)(panel B). The nonspecific portion was estimated under excess (50 nM) conditions and has been subtracted. Each value was normalized with respect to the initial applied concentration in the basal medium and represents the mean±S.E. of three independent experiments. Panel C shows the kinetic profiles, up to 10 min after the start of the chase period, obtained in different experiments. The vertical bar is not shown when the S.E. is smaller than the symbol.

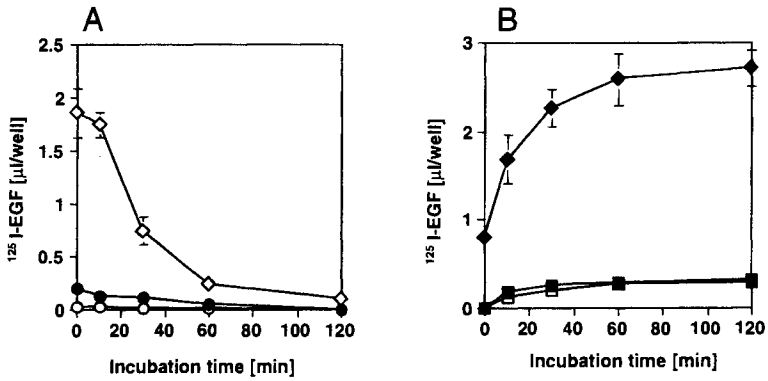

Fig. 4. Fate of internalized EGF in MDCK cells (pulse-chase study 2). A tracer amount of ^{125}I-EGF was applied to the basal medium, followed by a 2-hour incubation at 4°C. After extensive washing with ice-cold transport buffer (pH 7.2), the prewarmed buffer was applied to the monolayer, and the cells were further incubated for 20 min at 37°C. After washing with ice-cold transport buffer (pH 7.2) and then an acid buffer (pH 4.0) to strip surface-bound EGF, the prewarmed buffer was again applied to the monolayer which was incubated at 37°C. At designated times, the TCA-precipitable radioactivity in basal (■) and apical (□) medium was determined. After washing the cells, surface-bound ^{125}I-EGF the basal (●) and apical (○) sides and internalized ^{125}I-EGF (◇) were determined by the acid-washing technique. The TCA-soluble radioactivity in the cells and media were summed and shown as (◆). The nonspecific portion was estimated under excess (50 nM) conditions and has been subtracted. Each value was normalized with respect to the initial applied concentration in the basal medium and represents the mean±S.E. of three independent experiments.

conditions, of authentic ^{125}I-EGF (6.14×10^{-2} μl/mg protein) was comparable with that for the radioactivity appearing in the basal medium (8.66×10^{-2} μl/mg protein).

Fate of Internalized EGF (Pulse-Chase Study 3)

The acid-resistant and TCA-precipitable radioactivity at the start of the chase period was 2.17 ± 0.23 μl/well and fell with time (Fig. 5A). The degradation product increased in a time-dependent manner, reaching 2.15 ± 0.20 μl/well after the 2-hour chase period (Fig. 5B). TCA-precipitable radioactivity appearing in the apical medium during the 2-hour chase period was only 0.219 ± 0.030 μl/well (Fig. 5B). TCA-precipitable radioactivity also appeared in the basal medium, increasing in a time-dependent manner (Fig. 5B).

Integration Plots to Estimate Kinetic Parameters

The obtained k_{int} (0.221 ± 0.026 min^{-1}) was approximately seven times greater than k_{off} ($3.05 \pm 0.63 \times 10^2$ min^{-1}) (Fig. 6A, 6B). The k_{trans} ($2.74 \pm 0.37 \times 10^{-3}$ min^{-1}) was approximately 12 times less than the k_{deg} ($3.27 \pm 0.44 \times 10^{-2}$ min^{-1}) in pulse-chase study 1 (Fig. 6C, 6D). The k_{trans}, k_{deg}, and $k_{recycle}$ were $5.38 \pm 0.91 \times 10^{-3}$, $4.19 \pm 0.43 \times 10^{-2}$, and $4.20 \pm 0.89 \times 10^{-3}$ min^{-1}, respectively (Fig. 6E, 6F, 6G), in pulse-chase study 2 while the corresponding figures were $4.07 \pm 1.51 \times 10^{-3}$, $1.29 \pm 0.31 \times 10^{-2}$, and $4.48 \pm 0.28 \times 10^{-3}$ min^{-1}, respectively (Fig. 6H, 6I, 6J), in pulse-chase study 3.

DISCUSSION

To develop DDS involving RME to offer highly efficient drug targeting, it is important to regulate the intracellular fate of the endocytosed ligand and this can be achieved by a variety of methods (1–3). Kinetic analysis of the intracellular fate is useful for estimating the targetting efficiency. Since the transcytosis pathway can be used for the enhancement of systemic absorption as well as brain delivery, it is essential to develop a methodology to analyze each kinetic process, including receptor binding, internalization, intracellular sorting, and exocytosis, which affect the net amount transcytosed. In the present study, using several types of pulse-chase studies, we developed a kinetic model to describe the transcytosis of EGF (Fig. 7). Using this model, the rate-limiting step of the net transcytosis can be investigated.

Maratos-Flier *et al.* (4) reported that EGF is transcytosed only from basal to apical medium through binding to the EGF receptor on the basal surface. Such unidirectional transport was also found in the present study (Fig. 1). The difference in R_s between the basal and apical surfaces suggests that receptor density is much higher on the basal surface (Fig. 2). Brandli *et al.* (6) directly determined EGF receptors by immunoprecipitation using anti-EGF receptor antibody following enzymatic labeling of cell-surface proteins with [^{3}H] galactose and found that the EGF receptor is expressed on the basal surface while the degree of expression on the apical surface is negligible. Maratos-Flier *et al.* (4) performed a cross-linking study of ^{125}I-EGF to its receptor which suggested that the EGF receptor is expressed exclusively on the basal cell-surface. Thus, the EGF receptor is not expressed on the apical surface or is expressed at a very low level which cannot be easily detected.

To understand the reason for such unidirectional transcytosis of EGF, its intracellular fate also needs to be analyzed. In the present study, we performed three types of pulse chase studies in an attempt to clarify the validity of each kinetic

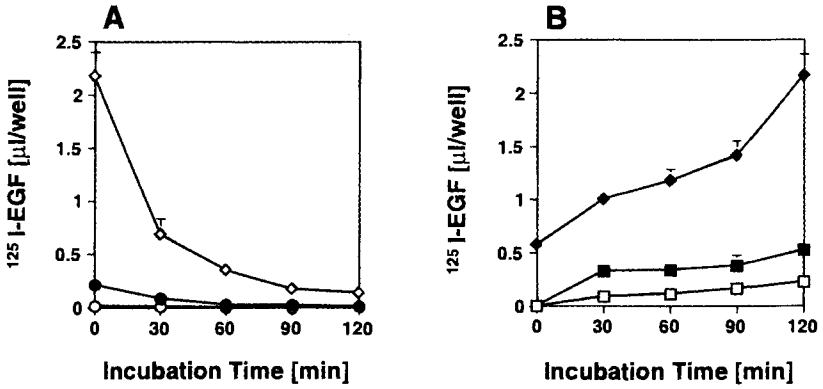

Fig. 5. Fate of internalized EGF in MDCK cells (pulse-chase study 3). A tracer amount of ^{125}I-EGF was applied to the basal medium, followed by a 20 min incubation at 37°C. After extensive washing with ice-cold transport buffer (pH 7.2) and also acid buffer (pH 4.0) to strip surface-bound EGF, the prewarmed buffer was applied to the monolayer which was then incubated at 37°C. At designated times, the TCA-precipitable radioactivity in basal (■) and apical (□) medium was determined. After washing the cells, surface-bound ^{125}I-EGF on the basal (●) and apical (○) sides and internalized ^{125}I-EGF (◇) were determined by the acid-washing technique. The TCA-soluble radioactivity in the cells and media were summed and shown as (◆). The nonspecific portion was estimated under excess (50 nM) conditions and has been subtracted. Each value was normalized with respect to the initial applied concentration in the basal medium and represents the mean±S.E. of three independent experiments.

parameter estimated. In our kinetic model, intracellular ligand was regarded as a single compartment (Fig. 7). However, it has been reported that endocytosed EGF is first sorted into the early endosome (compartment of uncoupling of receptor and ligand), followed by translocation into the late endosome (multivesicular body) (12). After that, EGF is degraded in the lysosome. Thus, the compartment for internalized ligand should include EGF molecules in several types of organella. Therefore, to obtain an insight into the validity of the kinetic analysis based on our mathematical model, these different types of pulse-chase studies were needed.

Kinetic analysis in pulse-chase study 1 revealed that 88% ($= k_{int}/(k_{int} + k_{off}) \times 100$) of surface-bound EGF is internalized while only a minor portion (12%) is dissociated from its receptor. The absolute value for k_{int} (0.221 min^{-1}) was comparable with that obtained in an isolated rat kidney perfusion system (11). In pulse-chase study 1 the TCA-precipitable radioactivity appeared in the apical medium in a time-dependent manner with a lag-time (Fig. 4B). This lag-time can be explained when we consider that it takes this time for EGF molecules to be taken up by the cells, undergo intracellular sorting and exocytosis into the apical medium. The cumulative amount of TCA-precipitable radioactivity appearing in the apical medium up to 120 min could account for only 6% of the surface-bound ^{125}I-EGF at the start of the chase period (Fig. 4). Thus, most of the EGF prebound to receptors on the basal surface passes into the lysosomes while a small portion is transferred to the apical medium.

In pulse-chase study 1, most of the ligand was located on the cell surface at the start of the chase period. Therefore, it is impossible to know if the ligand released into the basal medium comes from dissociation from the surface receptor or recycling from the cell interior. We designed pulse-chase studies 2 and 3 where most of the ligand was located inside the cells at the start of chase period. In these studies we found that the TCA-precipitable radioactivity appeared in the basal medium (Figs. 4, 5). The specific binding of this radioactivity to the membrane was comparable with that of authentic ^{125}I-EGF (see Results), demonstrating that intact EGF is recycled to the basal medium.

The absolute values of the kinetic parameters obtained in pulse chase studies 2 and 3 indicate that 63–81% ($k_{deg}/(k_{trans} + k_{deg} + k_{recycle}) \times 100$) of internalized EGF is transferred to lysosomes while 10–15% and 8–21% is transcytosed and recycled, respectively. Based on the kinetic model shown in Fig. 7, the transcytosis clearance (CL_{trans}) from basal to apical medium, designated as the initial velocity of the transcytosis rate divided by the ligand concentration, can be described by:

$$CL_{trans} = k_{on}R_{s,basal}(k_{int}/(k_{int} + k_{off}))(k_{trans}/(k_{trans} + k_{deg} + k_{recycle})) \quad (7)$$

When we consider that k_{int} is much greater than k_{off}, and k_{deg} is much greater than $k_{trans} + k_{recycle}$, Eq. (7) can be expressed simply by:

$$CL_{trans} = k_{on}R_{s,basal}k_{trans}/k_{deg} \quad (8)$$

Thus, surface-binding ($k_{on} \cdot R_{s,basal}$), degradation (k_{deg}), and exocytosis from cell interior to apical medium (k_{trans}) are rate-limiting steps in EGF transcytosis from basal to apical medium in MDCK epithelial cells.

When RME is used for enhancement of systemic absorption, the direction of transcytosis is contrary to that in the present study where we analyzed transcytosis of EGF from the basal to apical side. Nevertheless, the methodology shown in the present study can basically be applied to each vectorial transport. In transcytosis, most of the endocytosed ligand is usually translocated to lysosomes. Therefore, for the efficient systemic absorption and brain targeting via RME through polar-

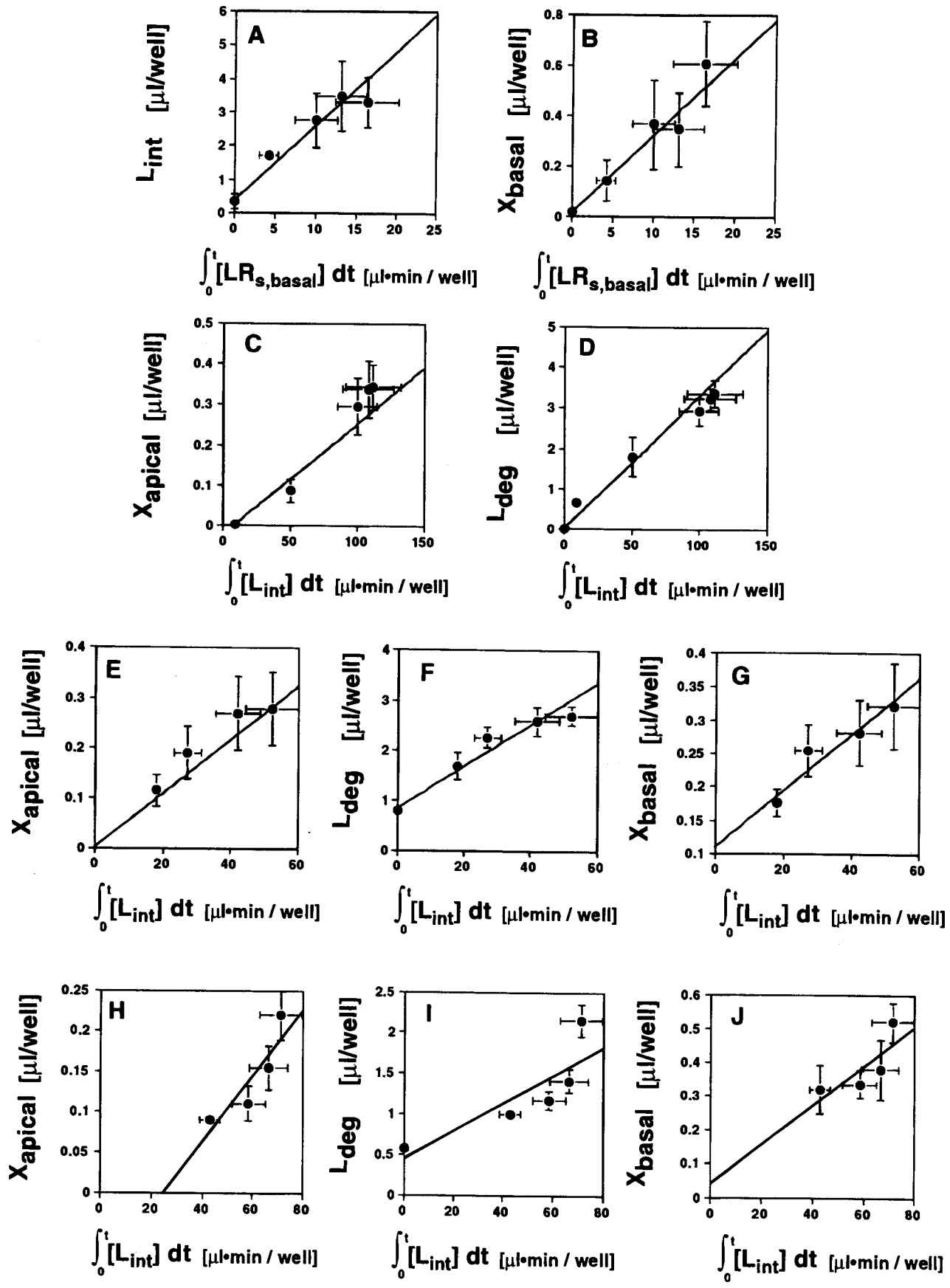
A
L_{int} [µl/well]
$\int_0^t [LR_{s,basal}]\,dt$ [µl•min / well]
B
X_{basal} [µl/well]
$\int_0^t [LR_{s,basal}]\,dt$ [µl•min / well]
C
X_{apical} [µl/well]
$\int_0^t [L_{int}]\,dt$ [µl•min / well]
D
L_{deg} [µl/well]
$\int_0^t [L_{int}]\,dt$ [µl•min / well]
E
X_{apical} [µl/well]
$\int_0^t [L_{int}]\,dt$ [µl•min / well]
F
L_{deg} [µl/well]
$\int_0^t [L_{int}]\,dt$ [µl•min / well]
G
X_{basal} [µl/well]
$\int_0^t [L_{int}]\,dt$ [µl•min / well]
H
X_{apical} [µl/well]
$\int_0^t [L_{int}]\,dt$ [µl•min / well]
I
L_{deg} [µl/well]
$\int_0^t [L_{int}]\,dt$ [µl•min / well]
J
X_{basal} [µl/well]
$\int_0^t [L_{int}]\,dt$ [µl•min / well]

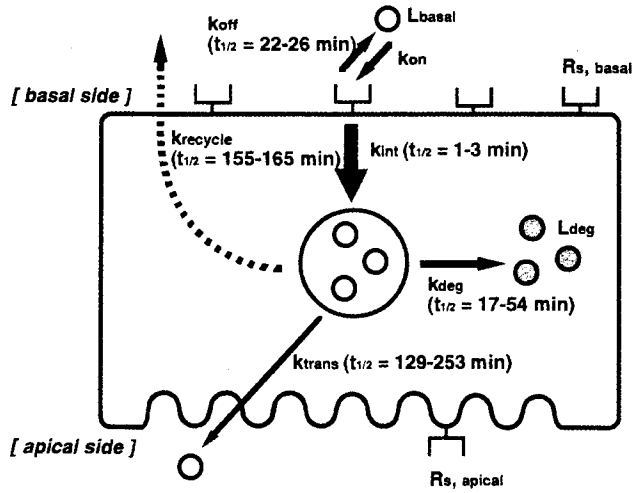

Fig. 7. Mathematical model describing the transcytosis of EGF in MDCK epithelial cells.

ized cells, we must develop some methodology to increase the transcytosis efficiency, avoiding lysosomal degradation. To this end, the kinetic analysis described in the present study may be a useful tool.

In conclusion, (i) most of the receptor-bound EGF on the basal surface is internalized rapidly, followed by gradual degradation. Exocytosis from cell interior to apical medium is a much slower process and one of the rate-limiting steps in EGF transcytosis; (ii) EGF is recycled into the basal medium after its internalization.

ACKNOWLEDGMENTS

We thank Mr. Hiroyuki Kusuhara for helpful suggestions. This study was supported in part by a Grant-in-Aid for Scientific Research provided by the Ministry of Education, Science and Culture of Japan.

REFERENCES

1. G. Molema and D. K. F. Meijer. *Adv. Drug Del. Rev.* **14**:25–50 (1994).
2. Y. Kato and Y. Sugiyama. *Crit. Rev. Ther. Drug Carrier Systems*, in press.
3. W. M. Pardridge. *Adv. Drug Del. Rev.* **15**:109–146 (1995).
4. E. Maratos-Flier, C. Y. Kao, E. M. Verdin, and G. L. King. *J. Cell Biol.*, **105**:1595–601 (1987).
5. J. Wan, M. E. Taub, D. Shah, and W. Shen. *J. Biol. Chem.* **267**:13446–13450 (1992).
6. A. W. Brandli, E. D. Adamson, and K. Simons. *J. Biol. Chem.* **266**:8560–8566 (1991).
7. H. Sato, Y. Sugiyama, Y. Sawada, T. Iga, S. Sakamoto, T. Fuwa, and M. Hanano. *Proc. Natl. Acad. Sci. USA.* **85**:8355–8359 (1988).
8. T. Nakamura, A. Tomomura, C. Noda, M. Shimoji, and A. Ichihara. *J. Biol. Chem.* **258**:9283–9289 (1983).
9. K. Yamaoka, Y. Tanigawara, T. Nakagawa, and T. Uno. *J. Pharm. Dyn.* **4**:879–885 (1981).
10. Y. Sugiyama and Y. Kato. In M. D. Taylor and G. L. Amidon (eds), *Peptide-Based Drug Design: Controlling Transport and Metabolism*, American Chemical Society Books Department, Washington, 1995, pp. 525–551.
11. D. C. Kim, M. Hanano, Y. Sawada, T. Iga, and Y. Sugiyama. *Am. J. Physiol.* **261**:F988–F997 (1991).
12. S. Jackle, E. A. Runquist, S. Miranda-Brady, and R. J. Havel. *J. Biol. Chem.* **266**:1396–1402 (1991).

Fig. 6. (*opposite*) Integration plots to estimate kinetic parameters (Panels A and B) Data obtained in pulse-chase study 1 were replotted using Eqs. (2) and (3) to estimate k_{int} and k_{off}, respectively. The straight lines represent the fitted lines using the data up to 10 min after the start of the chase period. (Panels C and D) Data obtained in pulse-chase study 1 were replotted using Eqs. (4) and (5) to estimate k_{trans} and k_{deg}, respectively. The straight lines represent the fitted lines using the data at 10, 20, 60, 90, and 120 min after the start of the chase period. (Panels E, F, and G) Data obtained in pulse-chase study 2 were replotted using Eqs. (4), (5), and (6) to estimate k_{trans}, k_{deg}, and $k_{recycle}$, respectively. The straight lines represent the fitted lines. The data at 10, 30, 60, and 120 min were used for the determination of k_{trans} and $k_{recycle}$ while those at 0, 10, 30, 60, and 120 min were used for the determination of k_{deg} (Panels H, I, and J). Data obtained in pulse-chase study 3 were replotted using Eqs. (4), (5), and (6) to estimate k_{trans}, k_{deg}, and $k_{recycle}$, respectively. The straight lines represent the fitted lines. The data at 30, 60, 90, and 120 min were used for the determination of k_{trans} and $k_{recycle}$ while those at 0, 30, 60, 90, and 120 min were used for the determination of k_{deg}.